

NASA Technical Memorandum 88994

NASA-TM-88994 19860021284

LATERAL STABILITY AND CONTROL DERIVATIVES EXTRACTED FROM
FIVE EARLY FLIGHTS OF THE SPACE SHUTTLE COLUMBIA

James R. Schiess

AUGUST 1986

FOR REFERENCE

NOT TO BE TAKEN FROM THIS ROOM

LIBRARY COPY

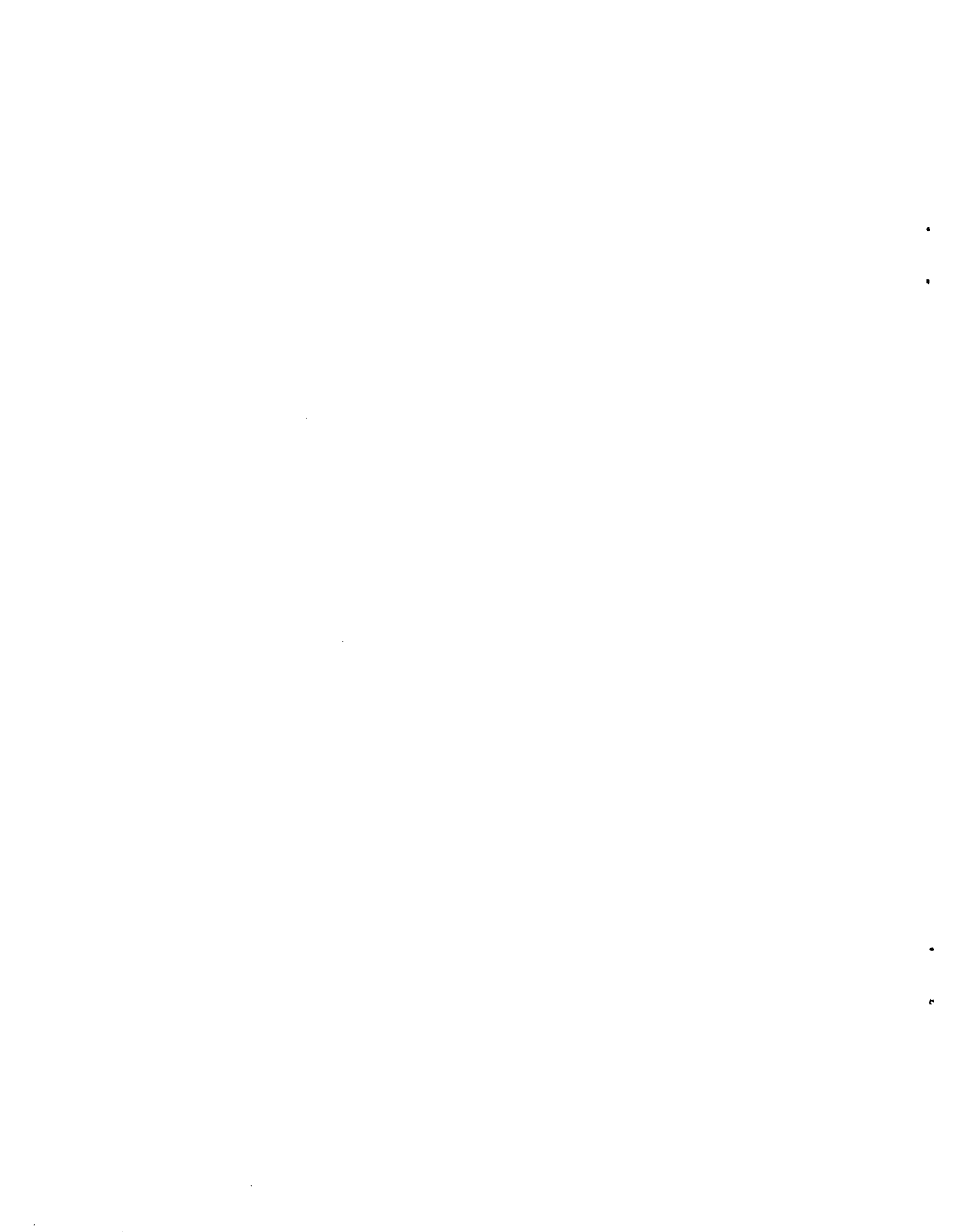
SEP 8 1986

LANGLEY RESEARCH CENTER
LIBRARY, NASA
HAMPTON, VIRGINIA

NASA

National Aeronautics and
Space Administration

Langley Research Center
Hampton, Virginia 23665



INTRODUCTION

One of the design requirements of the Space Transportation System (STS) vehicles dictated that the vehicles be capable of controlled flight during entry through the entire flow regime from free-molecule through hypersonic to subsonic flow. The resulting vehicle resembles in many ways a conventional aircraft in that it is a winged spacecraft with elevons, vertical tail, rudder and a body flap trim device. The elevons are used both for longitudinal pitch control, much like elevators, and for lateral control, like ailerons. These aerodynamic control surfaces are augmented with onboard reaction control pitch and yaw jets which are necessary for the low dynamic pressure regime.

Large quantities of wind-tunnel data were gathered during the design of the Space Shuttle. The accumulated data base describes the assumed aerodynamic characteristics of the Shuttle over a wide range of flight conditions. This data base, published in reference 1, will be called herein the preflight or data book values.

Six of the first nine Shuttle flights (STS-1, 2, 3, 4, 5 and 9) were flown by the Shuttle vehicle Columbia. The first five flights constituted the flight test plan of the Shuttle vehicle. Excluding flight one (STS-1), during which no lateral maneuvers designed for parameter extraction were performed, 31 Programmed Test Input (PTI) lateral maneuvers were made during these flights.

The 31 lateral maneuvers constitute a data base from which the stability and control derivatives are extracted. Because of safety constraints, the maneuvers are not optimal for parameter extraction; however, they are the best available flight data for the purposes of this study. The flight extracted values are compared to preflight values from reference 1. This paper presents results which are a part of ongoing research at Langley Research Center (LaRC)

to analyze the aerodynamics of the Shuttle vehicle (refs. 2 - 7) and is a companion to reference 8 which presents an analysis of longitudinal maneuvers performed by Columbia on the same five flights.

SYMBOLS

a_y	acceleration in y-direction, g units
b	wing span, m
C_{ℓ}	rolling-moment coefficient, $M_x/\bar{q}S_w b_w$
$C_{\ell,0}, C_{n,0}$	aerodynamic moments for trimmed flight
C_n	yawing-moment coefficients, $M_z/\bar{q}S_w b_w$
$C_{Y,0}$	aerodynamic force for trimmed flight
C_Y	lateral-force coefficient, $F_Y/\bar{q}S_w$
e	vector of measurement error
F	vector function representing equations of motion
g	acceleration due to gravity, 9.81 m/sec^2
G	vector function representing measurement equations
I_x, I_y, I_z, I_{xz}	moments of inertia
J	cost function
k	number of data points
L	likelihood function
m	mass, kg
p	roll rate, rad/sec
q	pitch rate, rad/sec
\bar{q}	dynamic pressure, $\rho V^2/2$, Pa
Q	vector of unknown parameters
r	yaw rate, rad/sec
R	measurement noise covariance matrix
S	wing area, m^2

t time, sec
 u velocity along X-body axis, m/sec
 U input vector
 v velocity along Y-body axis, m/sec
 V airspeed, m/sec
 w velocity along Z-body axis m/sec
 X vector of states
 X, Y, Z longitudinal, lateral, and vertical body axes
 Y vector of outputs
 α angle of attack, rad
 β sideslip angle, rad
 δa aileron deflection, rad
 δr rudder deflection, rad
 δRCS RCS control term, number of jets firing
 θ pitch angle, rad
 ϕ roll angle, rad
 $\dot{\phi}_0$ bias on roll rate, rad/sec

Subscripts:

i quantity at i^{th} time
 M measured quantity
 p, r rotary derivatives
 β static derivatives with respect to β
 $\delta a, \delta r, \delta RCS$ control derivatives with respect to indicated quantity
 t trimmed value

Matrix exponents:

T transpose of matrix
 -1 inverse of matrix

Mathematical notation:

- ^ estimated quantity when over symbol
- derivative with respect to time when over symbol
- ∇ gradient operator

Abbreviations:

ACIP	Aerodynamic Coefficient Identification Package
BET	Best Estimated Trajectory
IMU	Inertial Measurement Unit
DFI	Development Flight Instrumentation
LaRC	Langley Research Center
MMLE3	Modified Maximum Likelihood
PTI	Programmed Test Input
RCS	Reaction Control System
RGA,AA	Rate Gyro Assembly, Accelerometer Assembly
STS	Space Transportation System

Test Vehicle

The orbiter configuration is shown in figure 1 and key physical characteristics are given in table 1. The thick, double delta wing is configured with full span elevons, comprised of two panels per side. Each elevon panel is independently actuated. All four panels are deflected symmetrically as an elevator for pitch control, and left and right elevons are deflected differentially as an aileron (δa) for roll control.

The body flap is used as the primary longitudinal trim device. The elevons are programmed in conjunction with the body flap to follow a set schedule to provide the desired aileron effectiveness.

The vertical tail consists of the fin and a split rudder. The rudder panels are deflected symmetrically for yaw control and are separated to act as a speed brake to provide for subsonic energy modulation. The speed brake opens fully (87.2 degrees) just below Mach 10 and then follows a predetermined schedule until Mach 0.9 is reached. The rudder is not activated until Mach 5.

Stability augmentation is provided by the aft reaction control system (RCS) jets, with the forward jets reserved for on-orbit attitude control and for aborts. The aft yaw jets are active until Mach 1, while the pitch and roll jets are terminated at a pressure of 20 and 10 pounds per square foot, respectively. Additional details of the Shuttle vehicle and its systems are given in reference 1.

Maneuvers

During flights STS-2 through 5 and STS-9, especially designed maneuvers were performed to obtain data for use in extracting aerodynamic parameters. These maneuvers were performed to obtain data at specific points during the descent trajectory. The test points were chosen so that aerodynamic parameters could be determined along the descent trajectory to verify the aerodynamic model obtained from the wind tunnel tests. This verification procedure will add confidence to the assumed aerodynamics of the Shuttle where there is agreement and will point to areas of potential inaccuracy where there is no agreement.

The actual forms of the inputs to be performed were developed using a Shuttle simulation to generate responses for various inputs and then extracting parameters from these responses. The control inputs that gave the best definition of the parameters of interest were then used for the flight tests. In spite of the care taken to design effective inputs, because the automatic control system was active, the controls were coupled and the resulting re-

sponses were reduced in magnitude and correlated with each other and the control inputs. This led to identifiability problems and correlation of parameters during the extraction process. Additional details on the maneuver design are given in reference 9.

Instrumentation and Data Processing

As a development vehicle, the Shuttle is fully instrumented and has a number of redundant systems for measuring various vehicle states and controls. The instrument packages will be mentioned specifically. First is the Aerodynamic Coefficient Identification Package (ACIP), an instrumentation package specifically designed to measure rates, and accelerations and control surface positions required for parameter identification. The ACIP data was recorded at 172 samples per second. Second is the instrumentation for the flight guidance and control system, the Rate Gyro Assembly, and Accelerometer Assembly (RGA,AA), which is a source for acceleration and rate measurements. The RGA,AA data is recorded at 25 samples per second but is very noisy. The third source of flight measurements is the navigation instrumentation, the Inertial Measurement Unit (IMU). The IMU measurements are high fidelity but are recorded at only one sample per second which limits their usefulness.

With the exception of STS-2, for which ACIP data was not available because of recorder failure, the ACIP data was the primary source for the linear and angular accelerations, angular rates and control surface deflections. The RCS chamber pressures were used to determine the jet thrust, and these measurements came from the vehicle operational instrumentation.

The data considered most reliable was used to generate a best estimated trajectory (BET) for the Shuttle vehicle. The data written to tapes for the parameter extraction consisted of only those maneuvers considered appropriate for extraction. The linear and angular rates and control surface deflections

came from the ACIP instrumentation except for STS-2, where a combination of IMU and RGA,AA data was used. The BET angular rates and linear accelerations at the start of a maneuver were taken as initial conditions, and the rates and accelerations were integrated over time to obtain angular positions and vehicle velocities. The velocities were then corrected for the effect of winds, and the resulting components were used to calculate the vehicle total velocity, angle-of-attack and angle-of-sideslip. This combined data set is recorded at 25 samples per second and comprises the data contained on the tape to be processed by the parameter extraction software. Additional details on the instrumentation and data processing can be found in references 10, 11 and 12.

Equations of Motion

The lateral-direction equations of motion used in this study are based on perturbations about trimmed flight conditions and are written relative to the body axes shown in figure 1. The equations are

$$\dot{\beta} = \frac{\bar{q}S}{mV} (C_Y + \dot{\beta}_0) + \frac{g}{V} \cos \theta \sin \phi + p \sin \alpha - r \cos \alpha \quad (1)$$

$$\dot{p} = \frac{I_{XZ}}{I_X} \dot{r} + \frac{I_Y - I_Z}{I_X} qr + \frac{I_{XZ}}{I_X} pq + \frac{\bar{q}Sb}{I_X} C_{\ell} \quad (2)$$

$$\dot{r} = \frac{I_{XZ}}{I_Z} \dot{p} + \frac{I_X - I_Y}{I_Z} pq - \frac{I_{XZ}}{I_Z} qr + \frac{\bar{q}Sb}{I_Z} C_n \quad (3)$$

$$\dot{\phi} = p + r \cos \phi \tan \theta + \sin \phi \tan \theta + \dot{\phi}_0 \quad (4)$$

where

$$C_Y = C_{Y_0} + C_{Y_\beta} + C_{Y_p} \frac{pb}{2V} + C_{Y_r} \frac{rb}{2V} + C_{Y_{\delta r}} (\delta r - \delta r_t) + C_{Y_{\delta a}} (\delta a - \delta a_t) + C_{Y_{\delta RCS}} \delta RCS \quad (5)$$

$$C_\lambda = C_{\lambda_0} + C_{\lambda_\beta} + C_{\lambda_p} \frac{pb}{2V} + C_{\lambda_r} \frac{rb}{2V} + C_{\lambda_{\dot{\beta}}} \frac{\dot{\beta}b}{2V} + C_{\lambda_{\delta r}} (\delta r - \delta r_t) + C_{\lambda_{\delta a}} (\delta a - \delta a_t) + C_{\lambda_{\delta RCS}} \delta RCS \quad (6)$$

$$C_n = C_{n_0} + C_{n_\beta} + C_{n_p} \frac{pb}{2V} + C_{n_r} \frac{rb}{2V} + C_{n_{\dot{\beta}}} \frac{\dot{\beta}b}{2V} + C_{n_{\delta r}} (\delta r - \delta r_t) + C_{n_{\delta a}} (\delta a - \delta a_t) + C_{n_{\delta RCS}} \delta RCS \quad (7)$$

The results of this study are based on maneuvers performed at velocities of Mach 1 and higher. For this reason the terms containing velocity are sufficiently small that the equations of motion are considered essentially insensitive to the rotary derivatives and to $C_{\lambda_{\dot{\beta}}}$ and $C_{n_{\dot{\beta}}}$; therefore, these derivatives are fixed at zero throughout this study.

Time histories of five measured quantities were fit during the estimation process. These are the sideslip angle (β), roll and yaw rates (p, r), lateral acceleration (a_y) and bank angle (ϕ).

Maximum Likelihood Estimation

Stability and control derivatives were extracted using the maximum likelihood estimator. Among other statistical properties, the maximum likelihood estimator is efficient and asymptotically unbiased. This estimator consists

of maximizing the likelihood function of the measurement errors, which is the product of the probability density functions evaluated at each measurement time. This approach requires that the form of the measurement error distribution is known; it is normally assumed this distribution is Gaussian.

It is assumed the actual system can be modeled as

$$\dot{x}(t) = F(X,U,Q,t) \quad (8)$$

$$Y(t_i) = G(X,U,Q,t_i) + e_i, \quad i = 1,2,\dots,k \quad (9)$$

where equation (8) is a vector representation of equations (1) to (4) and equation (9) is a vector representation of the measurements. In these equations, X is the state vector, U the vector of controls, Q the vector of stability and control derivatives, t is time and e_i the vector of measurement noise for the measurements at time t_i .

If it is assumed that the measurement noise is Gaussian, then the likelihood function (ref. 13) is

$$L(Y,Q) = [(2\pi)^4 R]^{-k/2} \exp\left\{-\frac{1}{2} \sum_{i=1}^k [Y_M(t_i) - Y(t_i)]^T R^{-1} [Y_M(t_i) - Y(t_i)]\right\} \quad (10)$$

where the subscript M denotes actual measurements and R is the measurement covariance matrix. Taking the natural logarithm of equation (10) and multiplying by -1 yields the cost function

$$J(Q) = -\log L(Y,Q) = \frac{1}{2} \sum_{i=1}^N [Y_M(t_i) - Y(t_i)]^T R^{-1} [Y_M(t_i) - Y(t_i)] \\ + \frac{N}{2} \log R + 2N \log 2\pi \quad (11)$$

Maximization of equation (10) with respect to Q is equivalent to minimization of equation (11) with respect to Q . The last term on the right is constant relative to Q and can be neglected; if R is known, the second term can also be neglected for the same reason. Minimization of the remaining term results in solving $\nabla J_{Q=\hat{Q}} = 0$ which gives the estimates

$$\hat{Q}_{j+1} = \hat{Q}_j - [\nabla^2 J(\hat{Q}_j)]^{-1} \nabla J(\hat{Q}_j), \quad j = 0, 1, 2, \dots \quad (12)$$

Since a sequence of estimates, \hat{Q}_j , are obtained iteratively, the process must begin with initial parameter estimates, \hat{Q}_0 .

If R is unknown in equation (11), direct minimization of $J(Q)$ with respect to Q and R is complicated by the fact that R is an implicit function of Q . A simpler approach is to minimize with respect to Q and R independently. Minimization of equation (11) with respect to R yields

$$\hat{R} = \frac{1}{N} \sum_{i=1}^N [Y_M(t_i) - Y(t_i)] [Y_M(t_i) - Y(t_i)]^T \quad (13)$$

The procedure used here is, first, assuming \hat{R} is diagonal with initial estimates for the diagonal elements, iterate equation (12) several times. Then, on each succeeding iteration, first estimate \hat{R} using the most recent value of \hat{Q} in equations (9) and (13), and then apply equation (12) once using \hat{R} in $J(Q)$. This two-step process is repeated each iteration to convergence.

The computer software used to obtain the maximum likelihood estimates is MMLE3 (ref. 13). A detailed description of the software can be found in the reference.

Analysis and Results

In this section the results obtained in this study are discussed. These results are based on extracting the stability and control derivatives from 31 PTI maneuvers on the five flights. The time span for the measurements obtained during the maneuvers ranged from 4 to 15 seconds with the measurements sampled 25 times a second.

The estimation approach taken here is based on information contained in measured accelerations and rates, various trajectory parameters and the measured atmosphere. The method of analyzing atmospheric measurements which accounts for spatial, diurnal and semidiurnal corrections is described by Price (ref. 14). This atmospheric information is combined with onboard measurements of accelerations and rates in order to construct the trajectory (ref. 15) which is used for estimating the stability and control derivatives.

In the results presented, moment derivatives are relative to the flight center of gravity and were estimated with rotary derivatives fixed at zero and $C_{Y_{\delta a}}$ fixed at the data book value of 0.00042 per degree. All mass properties and center of gravity information were supplied by NASA Johnson Space Center and are shown in table 1. The weighting matrix (inverse of the measurement noise covariance matrix, \hat{R}) was initially set to a diagonal matrix with the value 796.3, 234.8, 4324, 237.5, and 21820. These values correspond, respectively, to the measured variables β , p , r , ϕ , and a_y . Estimation of \hat{R} using equation (13) began on iteration 4 for each maneuver; from 8 to 20 iterations were required for convergence.

The extracted stability and control derivatives will be presented in figures as functions of Mach number. Both flight-extracted and predicted values along with variations associated with the predicted values will be shown. For example, figure 2 shows rolling moment due to sideslip angle as a

function of Mach number with the predicted values (P) and variations (V) indicated by solid lines, the extracted values by the symbol "+". The predicted values are based on data book values, corresponding to flight 5, which are the result of numerous preflight tests of Shuttle aerodynamics (ref. 1). The variations reflect uncertainties in the data book values; they are based on differences between flight and predicted results for previously researched aircraft and extrapolated to the Shuttle configuration.

Lateral-Directional Moment Derivatives

$C_{l\beta}$ -- Extracted values of the rolling moment due to sideslip are shown in figure 2. Except for a few outliers, the values fall within the variations. Above Mach 7 the flight results are slightly more positive than the predicted values, showing less stability than predicted. Similar results have been reported by Maine and Iliff (ref. 16) and Kirsten et al. (ref. 17). The estimates in the region above Mach 22 are generally based on maneuvers having low dynamic pressure ($\bar{q} < 10$ psf), making it difficult to estimate stability and control derivatives. This circumstance may partially account for the estimates lying outside the variation band.

Below Mach 7 the estimates are highly scattered. At the lowest Mach numbers, both aileron and rudder controls are simultaneously active. As presently configured, it is not possible to perform maneuvers which allow isolated control surface motions, thus making it difficult to accurately separate the effects of different surfaces. Significant differences in extracted coefficients have been noted between values when estimating rudder parameters versus not estimating rudder parameters for the same maneuver (ref. 4). Three points for which rudder parameters were not estimated are shown in figure 2. Generally, therefore, results below Mach 5 must be accepted with caution.

$C_{n\beta}$ -- Results for the yawing moment due to sideslip are shown in figure 3. This coefficient is similar to the rolling moment due to sideslip in that there is considerable scatter below Mach 7 and the estimates lie within the variation band above Mach 7. This coefficient tends to be less negative than predicted below Mach 7 and more negative with a general downward trend above Mach 7.

Lateral Control Derivatives

$C_{l\delta a}$ -- Figure 4 shows the results for the rolling moment due to aileron. Below Mach 7, the aileron tends to be less effective than predicted, although there is much less scatter than seen in the previous coefficients. Above Mach 7, aileron effectiveness tends to be greater than predicted. Except for four outliers, the extracted values all lie within the variations about the predicted values. Careful analysis indicates these four points should not be rejected, however, since they were estimated from flights 4 and 9 which are somewhat different from flight 5. Specifically, the preflight values for these two flights are comparable to the upper variation bound shown in the figure.

$C_{n\delta a}$ -- In general the coefficient of yaw due to aileron (fig. 5) tends to be less effective than predicted, although the vast majority of extracted values lie within the variations. Of the three outliers, the most negative value near Mach 24 is from flight 4 and the other two from flight 5. In contrast to the previous parameter, for this parameter the preflight values for all five flights are similar, hence, the outliers do lie outside the variation bands.

$C_{l\delta r}$ -- The rolling moment due to rudder is shown in figure 6. All the estimates lie within one variation of the data book values and show this derivative to be close to what was predicted. Since all but one value are less

than the data book, there is a suggestion that the rudder may be somewhat less effective than predicted, especially below Mach 2.5.

$C_{n_{\delta r}}$ -- Figure 7 shows the yawing moment due to rudder. All the flight values lie within one variation of the data book value. However, at Mach 1 the flight value may be more effective than predicted. In the Mach range 1.5 to 3, there is a definite tendency for the rudder to be less effective than predicted.

Side Force Derivatives

$C_{Y_{\delta a}}$ -- Generally, the side force derivatives are slightly more difficult to estimate because the signal input to the estimation program has a very small signal to noise ratio. In addition, force signals tend to look the same regardless of cause, and hence, it is difficult for the program to decompose the signal into causative components. Thus, since $C_{Y_{\delta a}}$ is very small (0.00042) compared to other force derivatives, it was not possible to get a consistent estimate of this derivative with high confidence. Further, $C_{Y_{\delta a}}$ appears to alias the RCS side force derivative when it is estimated.

Therefore, for all cases presented in this report $C_{Y_{\delta a}}$ was fixed at the data book value.

$C_{Y_{\beta}}$ -- Side force derivative with respect to sideslip angle is shown in figure 8. Of the five outliers, four are from flights 3, 4, and 9; the preflight values of this parameter on flights 3, 4, 5 and 9 are sufficiently similar to confirm that the four points are outliers. In contrast, the outlier near Mach 1.5 lies in a region of great uncertainty and may be a reasonable value. The remaining values are moderately scattered within the variation bounds. Both the outliers and the values within the variation bounds tend to be more positive than the data book values. This suggests the Shuttle vehicle is less stable than the data book indicates.

$C_{Y_{\delta r}}$ -- The side force due to rudder given in figure 9 indicates a considerable scatter in the estimates. Only two flight values lie within the variation bounds. These results are indicative of the aforementioned small signal to noise ratio in the onboard accelerometers and the ensuing difficulty in decomposing the signal. Accurate identification of the parameter does not appear possible with the data and estimation software used in this study.

RCS Derivatives

The RCS jets were treated in MMLE3 as if they were an additional aerodynamic control surface. The solutions were obtained throughout the speed range for side force, rolling moment and yawing moment derivatives due to yaw jet firings. In this paper, yaw jet evaluation is presented as a function of Mach number on a per jet basis. Comparisons are made to STS-4 preflight values based on known vacuum thrust corrected for altitude effects. Because the altitude profiles of the five flights are slightly different, the flight values will differ somewhat from the preflight values presented here. Furthermore, the preflight values have not been corrected for flow-field interactions.

$C_{Y_{RCS}}$ -- Side force due to yaw jet firing is shown in figure 10. The differences between predicted and flight values can be attributed to jet-interaction effects consisting of flow-field interactions and vehicle impingements, in addition to the aforementioned altitude profile differences. The figure shows good agreement between flight and predicted values with an indication that the yaw jets are somewhat more effective than predicted.

$C_{n_{RCS}}$ -- The flight values for the yawing moment due to yaw jets shown in figure 11 generally agree well with the predicted values. Considering the sources of differences noted previously, the yaw jets are less effective than predicted by not more than 10 percent.

$C_{\lambda_{RCS}}$ -- In the case of the rolling moment due to yaw jets shown in figure 12, the differences between flight and predicted values are significantly larger. This suggests greater interaction effects than seen in the previous two derivatives. The greater scatter in this derivative across the Mach range indicates there is also much more variability in the interactions. Verification of the interactions at a few points using the Development Flight Instrumentation (DFI) is given in reference 4. DFI pressure measurements on the upper wing surface from flights 3 and 5 were integrated spanwise and chordwise. The interaction calculated in this manner is then added to the predicted derivative; the resulting corrected derivatives, as shown in figure 12, compare very favorably with the flight values. Thus, it appears that the lower effectiveness of this derivative can be largely attributed to flow-field interactions which were not originally modeled in the preflight values.

CONCLUDING REMARKS

The lateral stability and control of the Columbia Shuttle orbiter has been analyzed over the hypersonic speed range from Mach 1 to 25. Acceleration and rate measurements made during 31 lateral maneuvers on flights 2, 3, 4, 5, and 9 were used in a maximum likelihood estimation computer program to extract aerodynamic coefficients. The flight-derived coefficients were compared to preflight data book values.

The extracted stability and control derivatives were usually within one variation of the preflight values, although the scatter is generally greater below Mach 5. Several coefficients were found to be somewhat less effective than predicted; this is particularly true for the aileron derivatives below Mach 7. The yaw jet results show these jets to be fully effective regarding side force. On the other hand, the yaw jets appear to be only about 90 percent effective in terms of the yawing and rolling moments. For the latter

derivative, the lower effectiveness is apparently due to flow-field interactions.

REFERENCES

1. Aerodynamic Design Data Book--Volume I: Orbiter Vehicle. NASA CR 160386, 1978.
2. Compton, Harold R.; Scallion, William I.; Schiess, James R.; and Suit, William T.: Shuttle Entry Performance and Stability and Control Derivatives Extraction from Flight Measurement Data. AIAA Paper No. 82-1317, 1982.
3. Suit, W. T.; Compton, H. R.; Scallion, W. I.; and Schiess, J. R.: Simplified Analysis Techniques to Support the Determination of Shuttle Aerodynamics. AIAA Paper No. 83-0117, 1983.
4. Compton, H. R.; Schiess, J. R.; Suit, W. T.; Scallion, W. I.; and Hudgins, J. W.: Evaluation of Shuttle Performance and Lateral Stability and Control over the Supersonic and Hypersonic Speed Range. NASA CP-2283, 1983.
5. Suit, William T.; Compton, Harold R.; Scallion, William I.; Schiess, James R.; and Gahan, L. Sue: Analysis of Shuttle Oscillation in the Mach Number = 1.7 to Mach Number = 1.0 Range. NASA CP-2283, 1983.
6. Schiess, J. R.: Suit, W. T.; and Scallion, W. I.: Investigation of the Effect of Vehicle, Angle-of-Attack, and Trim Elevon Position on the Lateral-Directional Aerodynamic Parameters of the Shuttle Orbiter. AIAA Paper No. 87-2072, 1984.
7. Suit, William T. and Schiess, James R.: Supplement to the Shuttle Aerodynamic Database Using Discovery Flight Tests. AIAA Paper No. 85-1765, 1985.
8. Suit, William T.: Summary of Longitudinal Stability and Control Parameters as Determined from Space Shuttle Columbia Flight Test Data. NASA TM 87768, July 1986.
9. Cooke, D. R.: Space Shuttle Stability and Control Test Plan. AIAA Paper No. 82-1315, 1982.
10. Findlay, J. T.; Kelly, G. M.; and Henry, M. W.: An Extended BET Format for LaRC Shuttle Experimenters: Definition and Development. NASA CR-165882, April 1982.
11. Findlay, J. T.; Kelly, G. M.; and McConnell, J. G.: An AERodynamic Best Estimate Trajectory File (AEROBET) for NASA Langley Research Center Shuttle Investigations. AMA Report 82-9, Analytical Mechanics Associates, Inc., March 1982.
12. Flanagan, P. F.: Final Report/GTFILE Generation - Definition and Development. AMA Report 81-20, Analytical Mechanics Associates, Inc., July 1981.

13. Maine, Richard E. and Iliff, Kenneth W.: User's Manual for MMLE3, a General FORTRAN Program for Maximum Likelihood Parameter Estimation. NASA TP-1563, 1980.
14. Price, Joseph M.: Atmospheric Definition for Shuttle Investigations. Journal of Spacecraft and Rockets, vol. 20, pp. 133-140, March-April 1983.
15. Compton, Harold R.; Findlay, John T.; Kelly, George M.; and Heck, Michael L.: Shuttle (STS-1) Entry Trajectory Reconstruction. AIAA Paper No. 81-2459, 1981.
16. Maine, R. E. and Iliff, K. W.: Selected Stability and Control Derivatives from the First Three Space Shuttle Entries. AIAA Paper No. 82-1318, 1982.
17. Kirsten, P. W.; Richardson, D. F.; and Wilson, C. M.: Predicted and Flight Test Results of the Performance, Stability and Control of the Space Shuttle from Reentry to Landing. Shuttle Performance: Lessons Learned Conference, NASA CP-2283, 1983.

TABLE 1. ENTRY PHYSICAL CHARACTERISTICS OF SPACE SHUTTLE COLUMBIA

Mass Properties (range for five flights):

Mass, kg 91,917 - 100,309

Moments of Inertia (range for five flights):

I_x , kg-m^2 1,171,428 - 1,313,633

I_y , kg-m^2 9,228,939 - 9,614,705

I_z , kg-m^2 9,584,958 - 10,031,878

I_{xz} , kg-m^2 205,832 - 223,189

Wing:

Reference area, m^2 249.91

Mean aerodynamic chord, m 12.06

Span, m 23.79

Elevon (per side):

Reference area, m^2 19.51

Mean aerodynamic chord, m 2.30

Rudder (per side panel):

Reference area, m^2 9.30

Mean aerodynamic chord, m 1.86

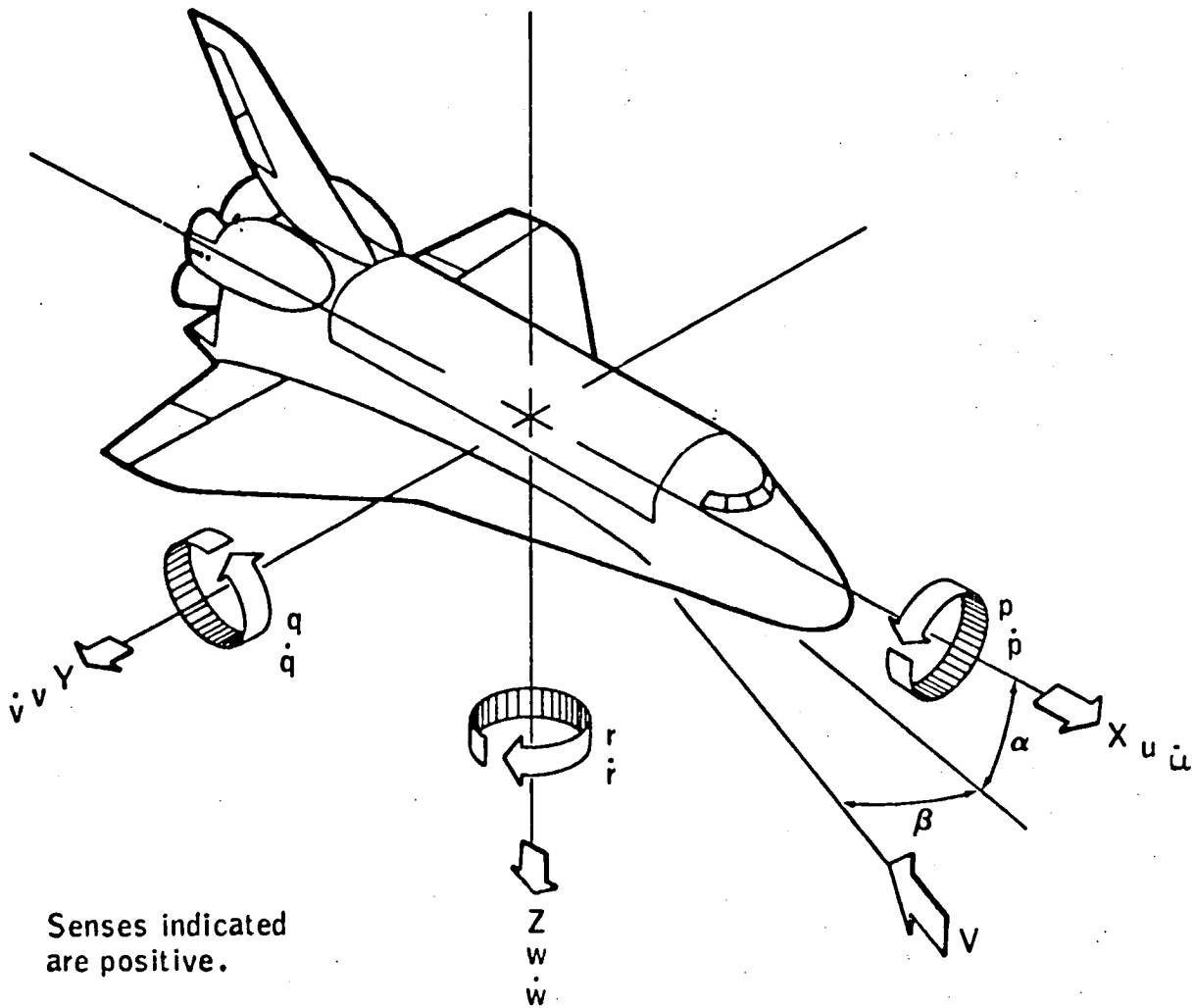


FIGURE 1.- SCHEMATIC OF STS BODY AXES.

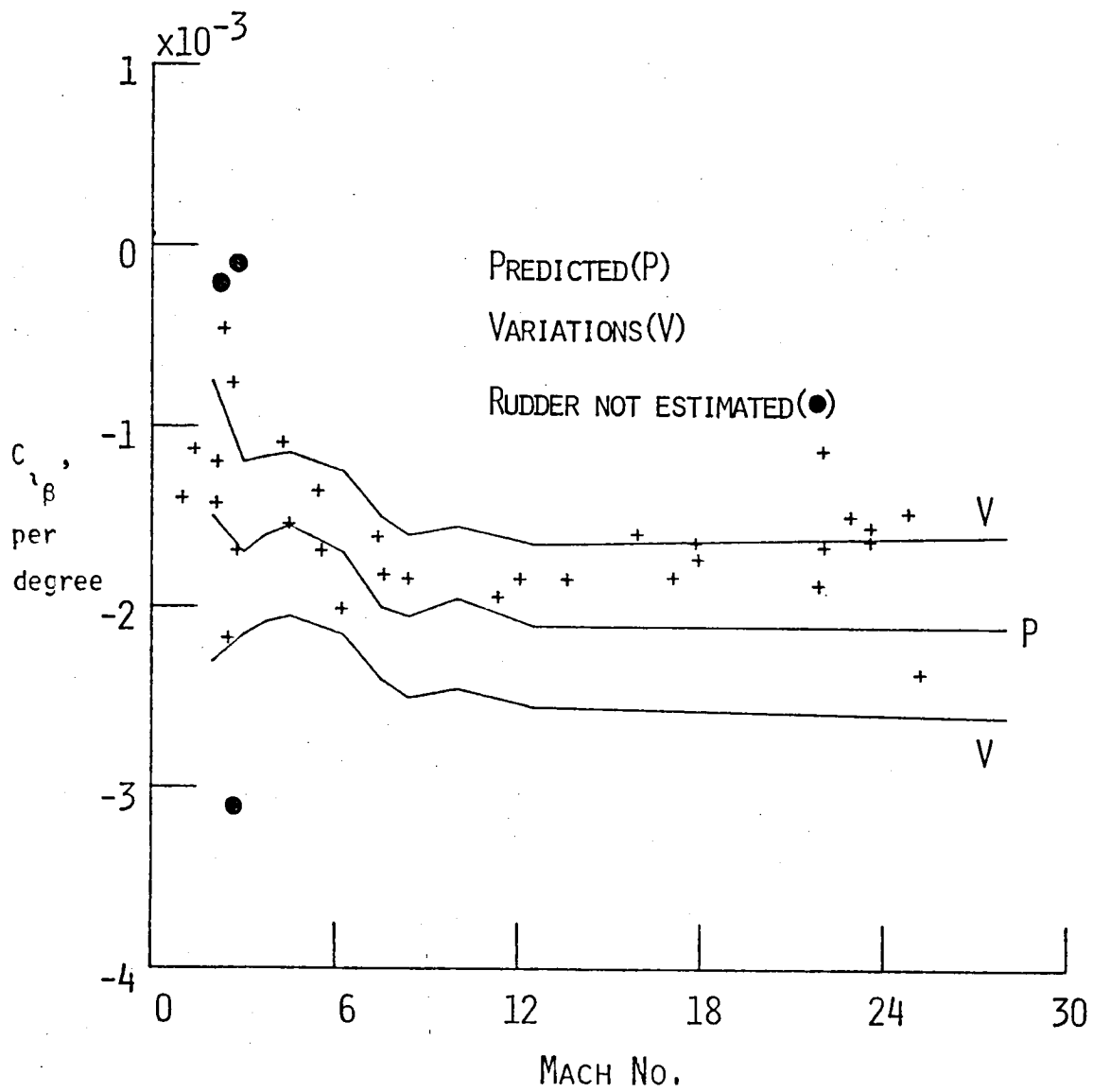


Figure 2.- Rolling moment due to sideslip versus Mach number

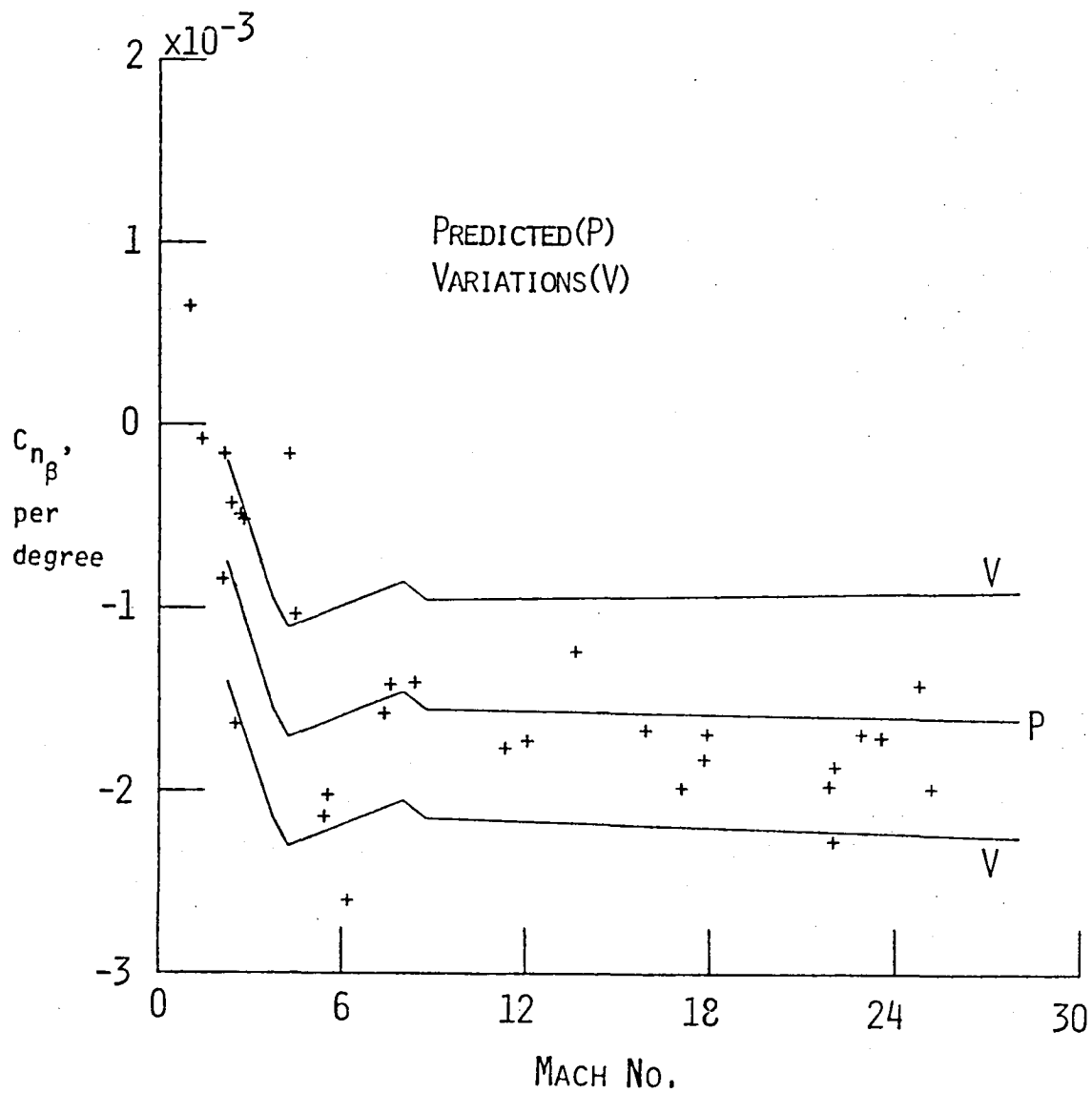


Figure 3.- Yawing moment due to sideslip versus Mach number.

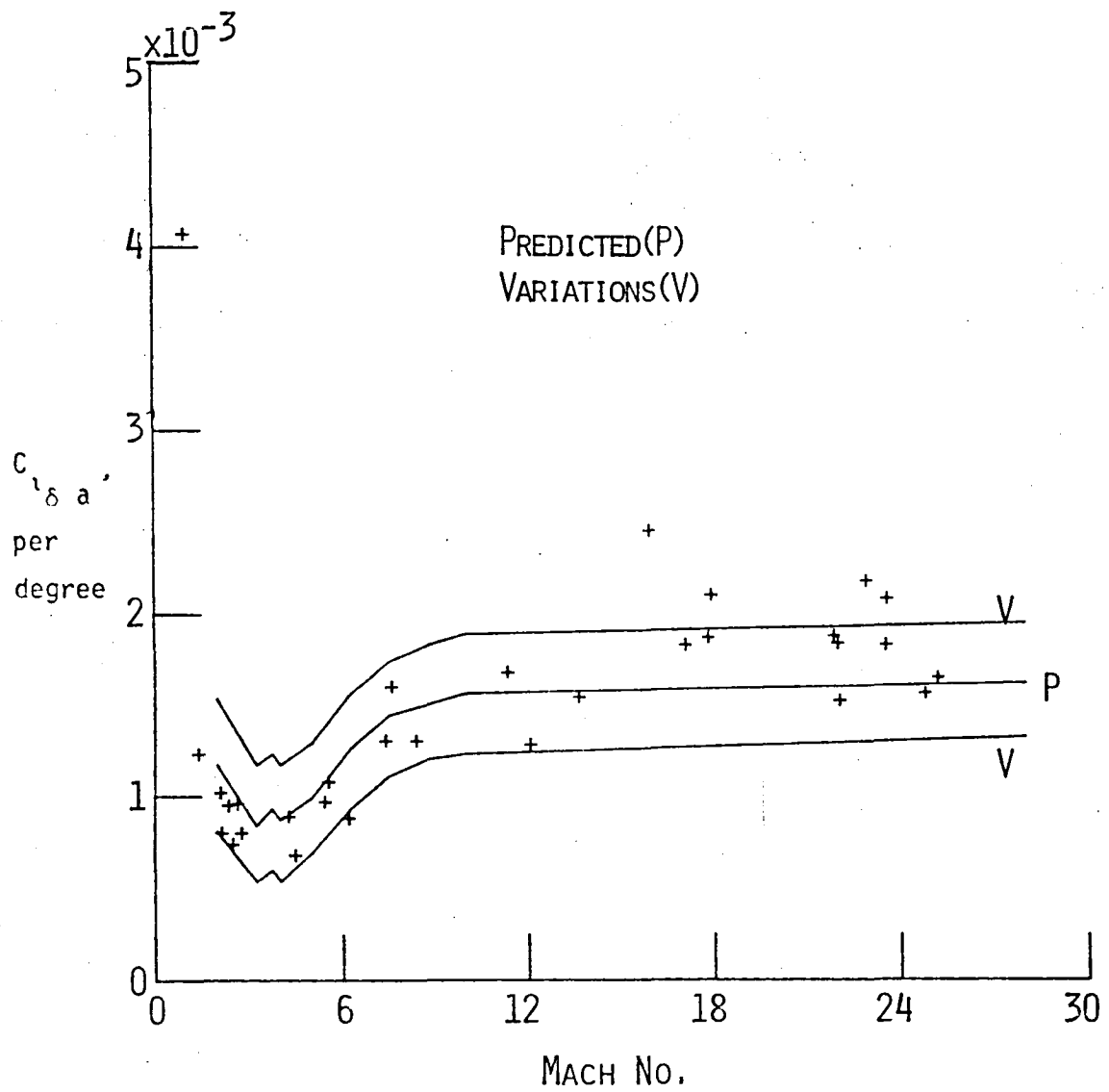


Figure 4.- Rolling moment due to aileron versus Mach number.

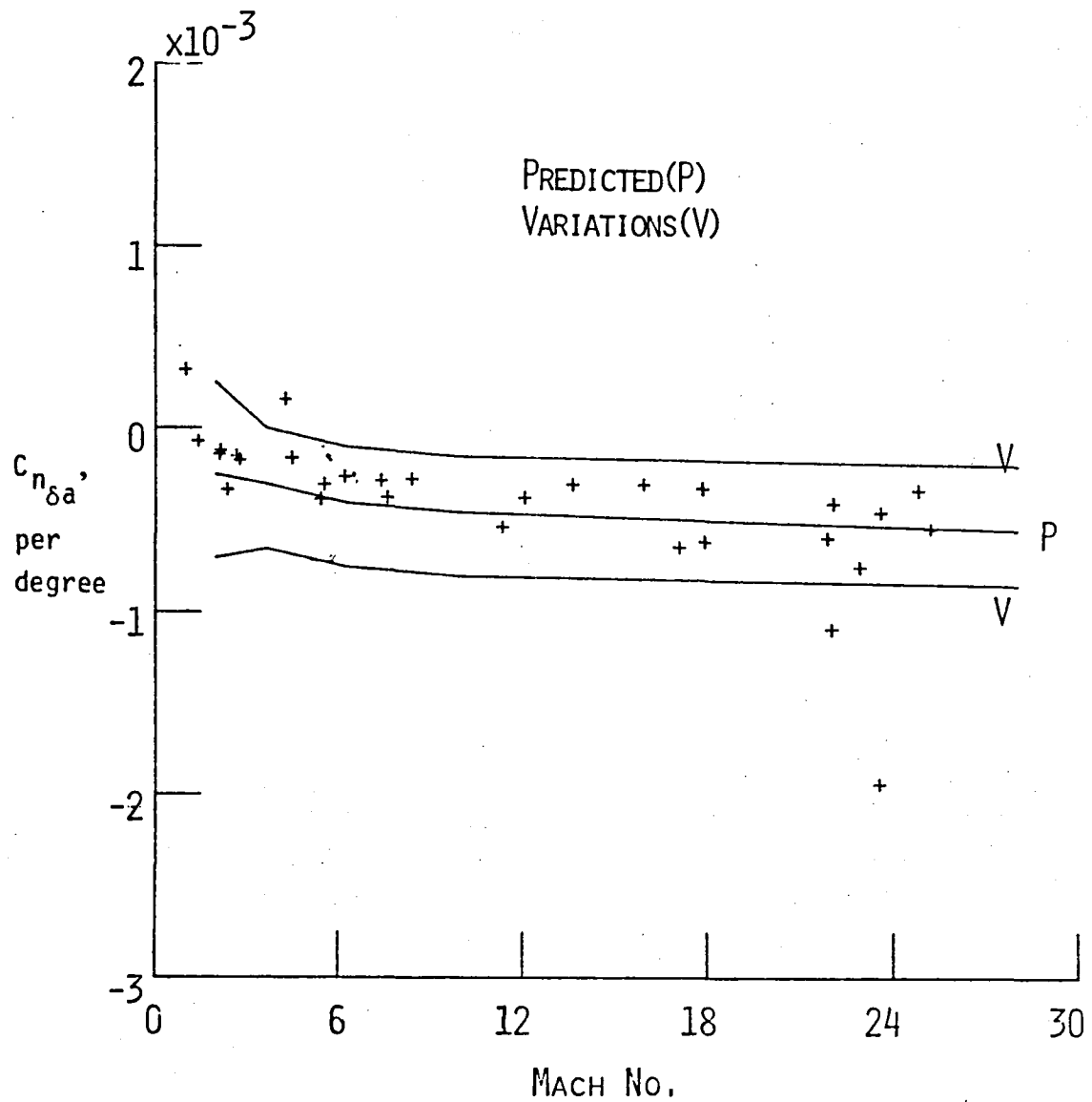


Figure 5.- Yawing moment due to aileron versus Mach number

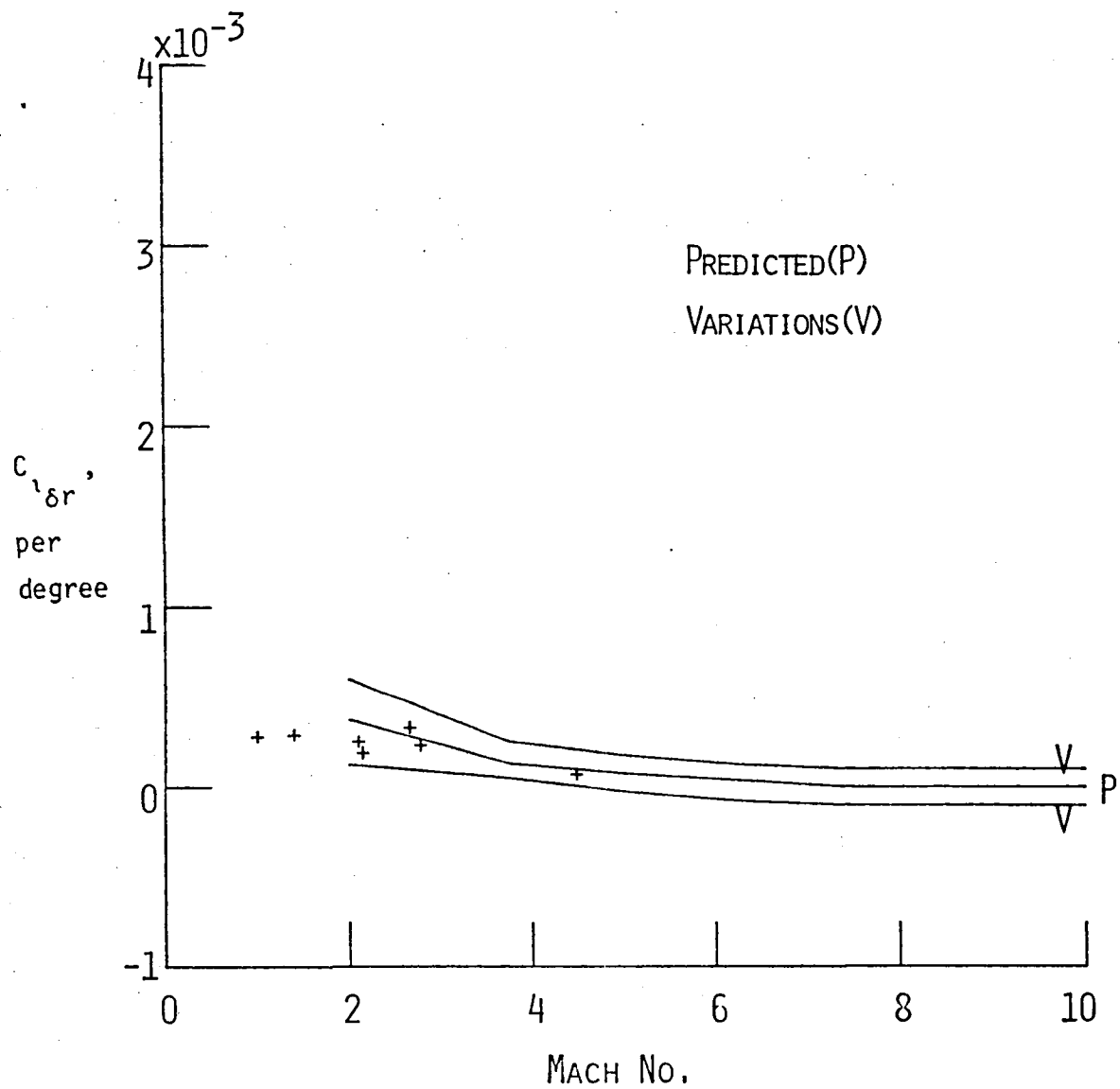


Figure 6.- Rolling moment due to rudder versus Mach number

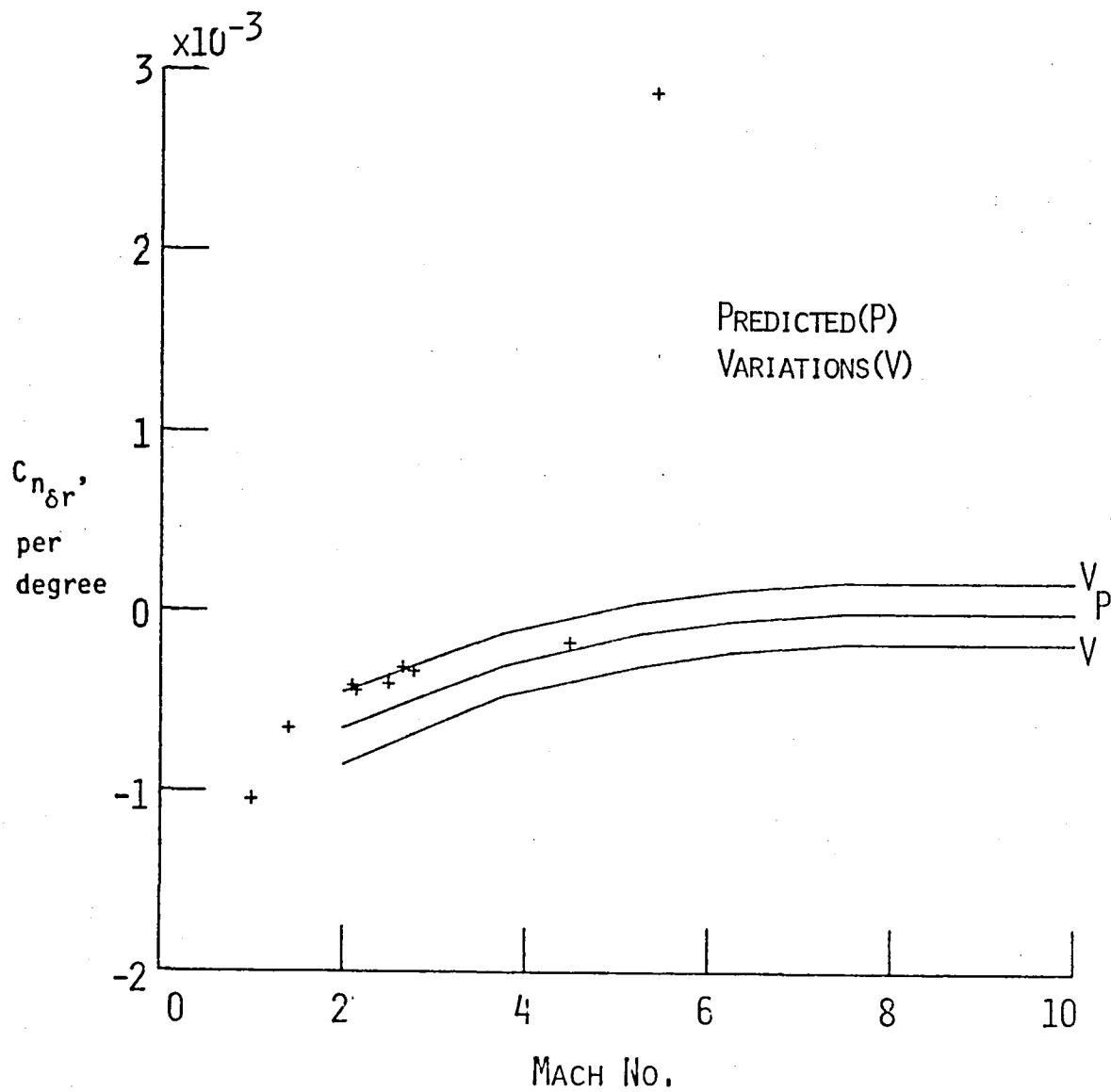


Figure 7.- Yawing moment due to rudder versus Mach number.

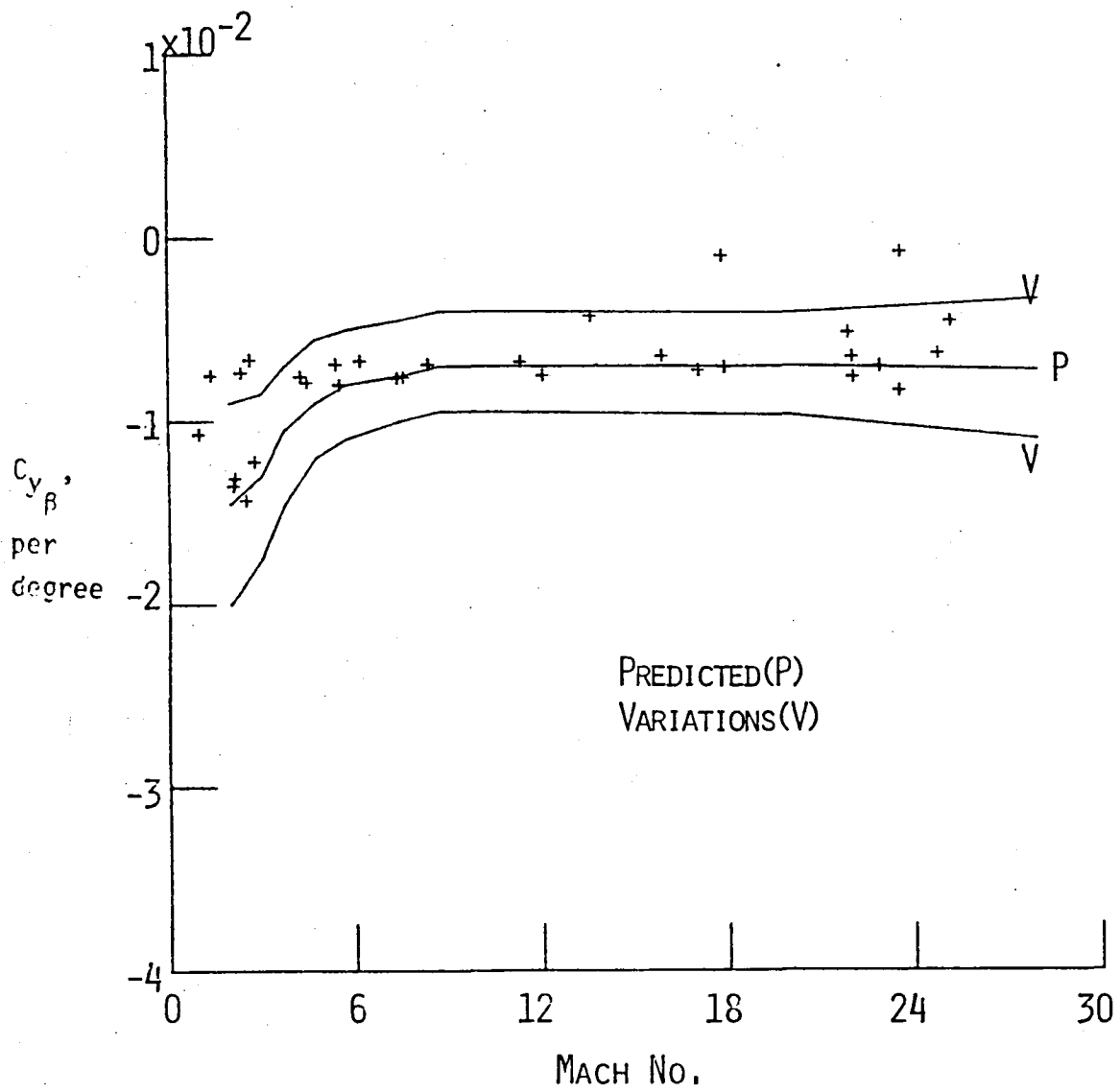


Figure 8.- Side force due to sideslip versus Mach number.

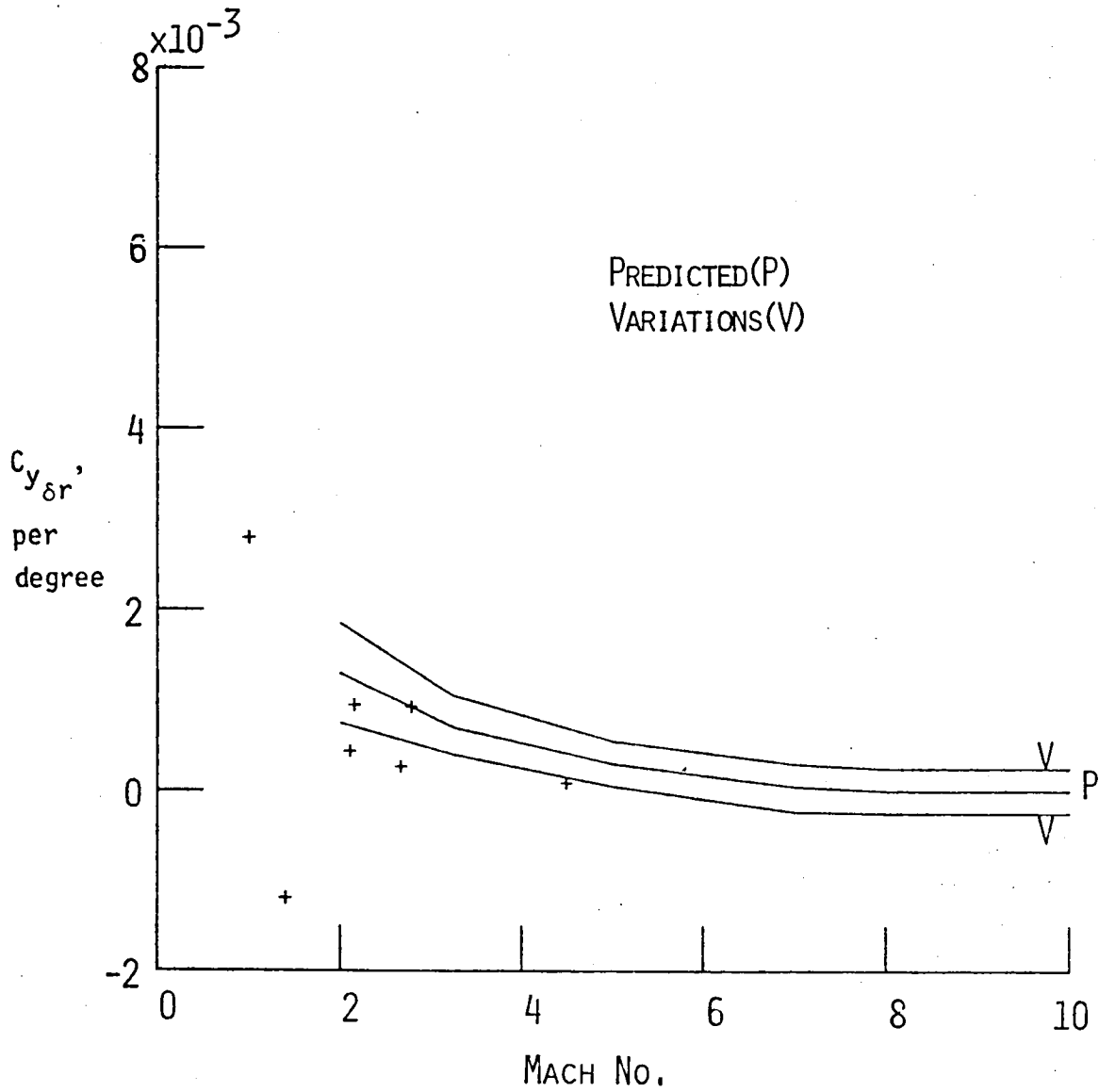


Figure 9.- Side force due to rudder versus Mach number.

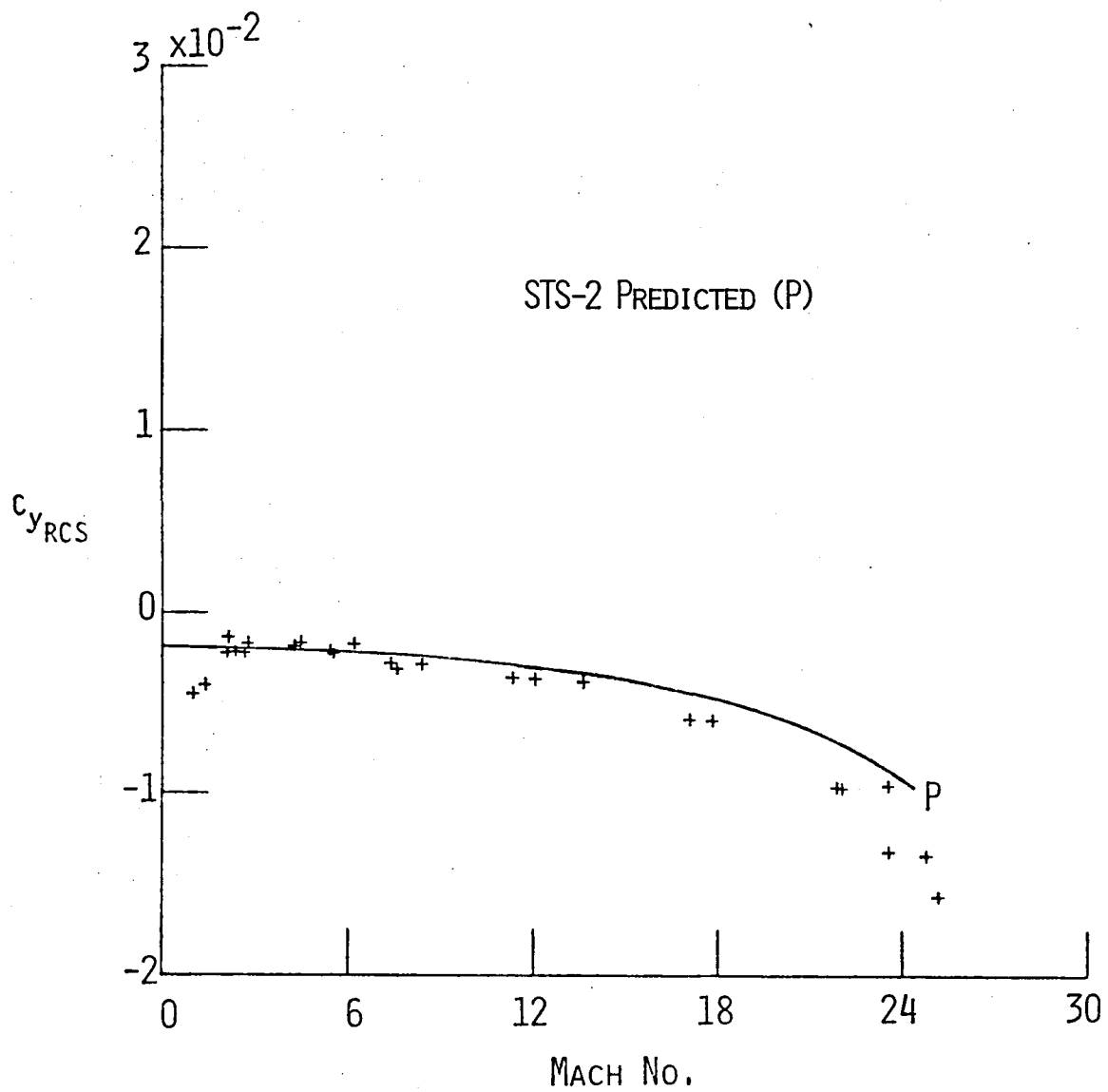


Figure 10.- Side force due to RCS versus Mach number.

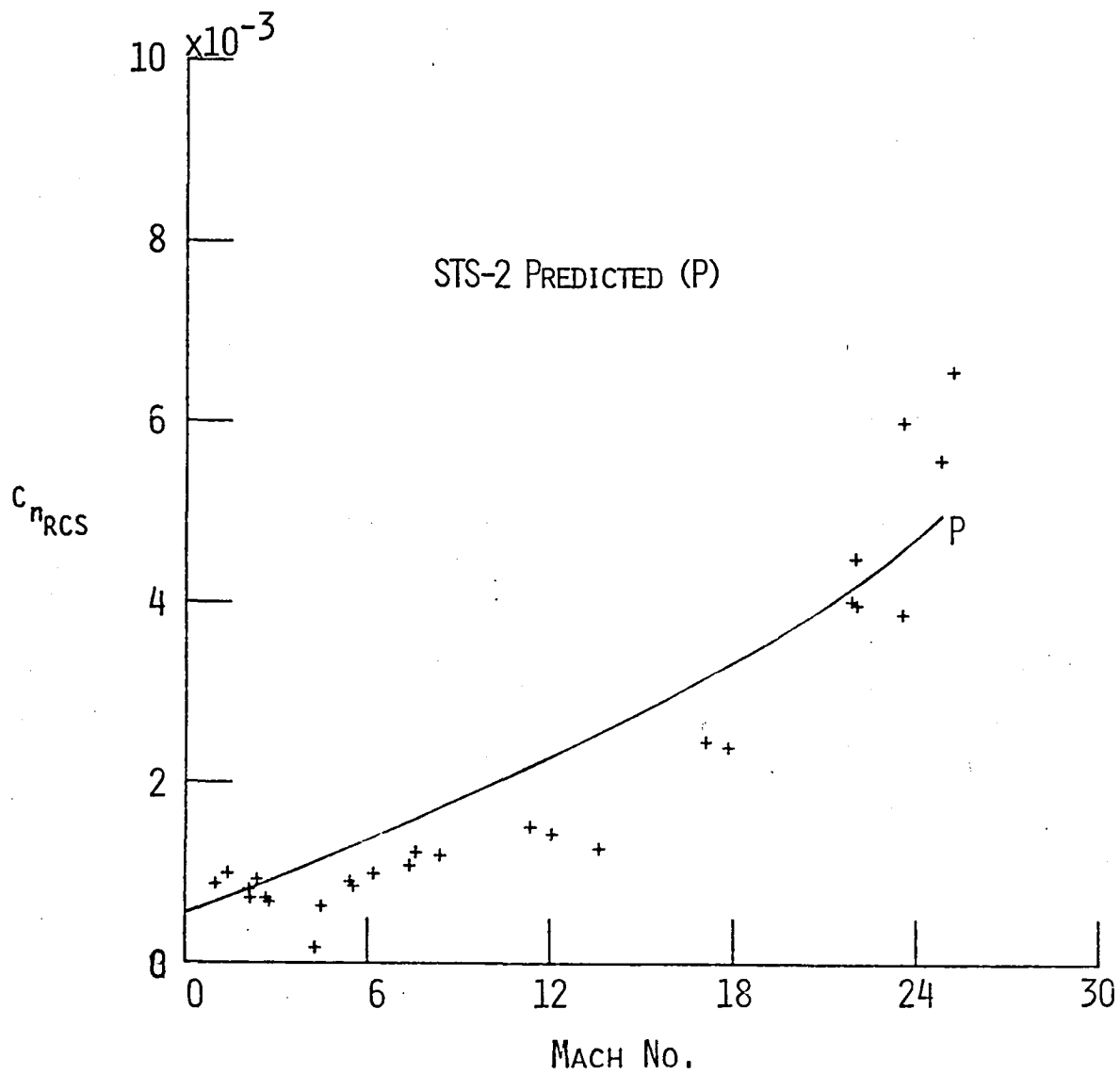


Figure 11.- Yawing moment due to RCS versus Mach number.

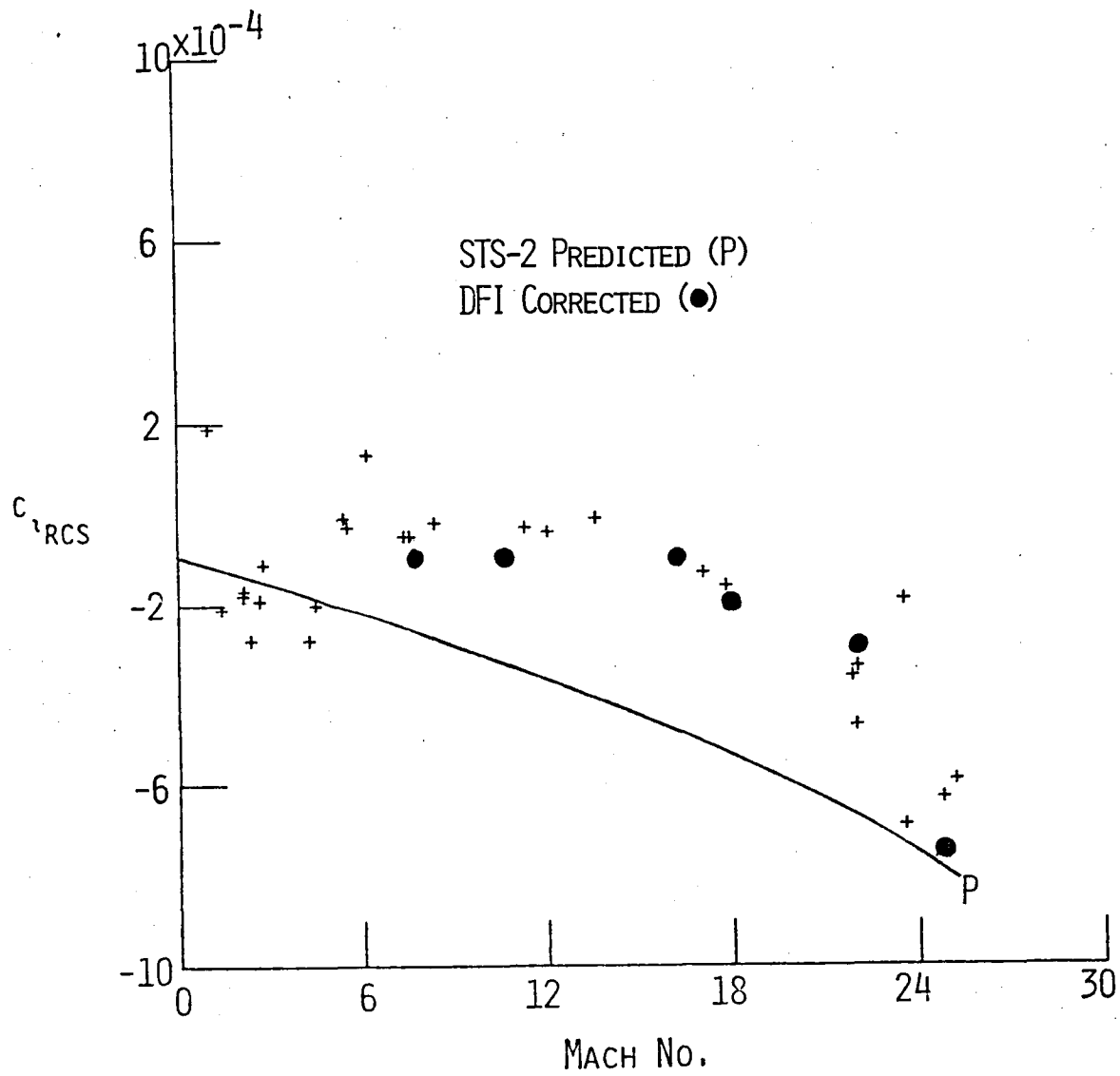


Figure 12.- Rolling moment due to RCS versus Mach number.



1. Report No. NASA TM-88994		2. Government Accession No.		3. Recipient's Catalog No.	
4. Title and Subtitle Lateral Stability and Control Derivatives Extracted from Five Early Flights of the Space Shuttle Columbia				5. Report Date August 1986	
				6. Performing Organization Code 506-40-11-03	
7. Author(s) James R. Schiess				8. Performing Organization Report No.	
9. Performing Organization Name and Address NASA Langley Research Center Hampton, VA 23665-5225				10. Work Unit No.	
				11. Contract or Grant No.	
12. Sponsoring Agency Name and Address National Aeronautics and Space Administration Washington, DC 20546-0001				13. Type of Report and Period Covered Technical Memorandum	
				14. Sponsoring Agency Code	
15. Supplementary Notes					
16. Abstract Flight data taken from the first five flights (STS-2, 3, 4, 5 and 9) of the Space Transportation System Shuttle Columbia during entry are analyzed to determine the Shuttle lateral aerodynamic characteristics. Maximum likelihood estimation is applied to data derived from accelerometer and rate gyro measurements and trajectory, meteorological and control surface data to estimate lateral-directional stability and control derivatives. The estimated parameters are compared across the five flights and to preflight predicted values.					
17. Key Words (Suggested by Author(s)) Maximum likelihood estimation Aerodynamic coefficients Atmospheric reentry			18. Distribution Statement Unclassified - Unlimited STAR Category - 16		
19. Security Classif. (of this report) Unclassified		20. Security Classif. (of this page) Unclassified		21. No. of Pages 33	22. Price A03

